THE LONG-TERM DYNAMICAL EVOLUTION OF DISK-FRAGMENTED MULTIPLE SYSTEMS IN THE SOLAR NEIGHBORHOOD

YUN LI[1,2], M. B. N. KOUWENHOVEN[3,4], D. STAMATELLOS[5], AND SIMON P. GOODWIN[6]
[1] Department of Astronomy, School of Physics, Peking University, Yiheyuan Lu 5, Haidian Qu, Beijing 100871, P. R. China
[2] Center for Astronomy and Astrophysics, Department of Physics and Astronomy, Shanghai Jiao Tong University, Shanghai 200240, P. R. China
[3] Department of Mathematical Sciences, Xi'an Jiaotong-Liverpool University, 111 Ren'ai Road, Suzhou Dushu Lake Science and Education Innovation District,
Suzhou Industrial Park, Suzhou 215123, P. R. China
[4] Kavli Institute for Astronomy and Astrophysics, Peking University, Yiheyuan Lu 5, Haidian Qu, Beijing 100871, P. R. China; t.kouwenhoven@xjtlu.edu.cn
[5] Jeremiah Horrocks Institute for Mathematics, Physics & Astronomy, University of Central Lancashire, Preston PR1 2HE, UK
[6] Department of Physics & Astronomy, The University of Sheffield, Hicks Building, Hounsfield Road, Sheffield S3 7RH, UK

ABSTRACT

The origin of very low-mass hydrogen-burning stars, brown dwarfs (BDs), and planetary-mass objects (PMOs) at the low-mass end of the initial mass function is not yet fully understood. Gravitational fragmentation of circumstellar disks provides a possible mechanism for the formation of such low-mass objects. The kinematic and binary properties of very low-mass objects formed through disk fragmentation at early times (<10 Myr) were discussed in our previous paper. In this paper we extend the analysis by following the long-term evolution of disk-fragmented systems up to an age of 10 Gyr, covering the ages of the stellar and substellar populations in the Galactic field. We find that the systems continue to decay, although the rates at which companions escape or collide with each other are substantially lower than during the first 10 Myr, and that dynamical evolution is limited beyond 1 Gyr. By $t = 10$ Gyr, about one third of the host stars are single, and more than half have only one companion left. Most of the other systems have two companions left that orbit their host star in widely separated orbits. A small fraction of companions have formed binaries that orbit the host star in a hierarchical triple configuration. The majority of such double-companion systems have internal orbits that are retrograde with respect to their orbits around their host stars. Our simulations allow a comparison between the predicted outcomes of disk fragmentation with the observed low-mass hydrogen-burning stars, BDs, and PMOs in the solar neighborhood. Imaging and radial velocity surveys for faint binary companions among nearby stars are necessary for verification or rejection of the formation mechanism proposed in this paper.

Key words: brown dwarfs – stars: formation – stars: kinematics and dynamics – stars: low-mass – planetary systems

1. INTRODUCTION

Low-mass stars and brown dwarfs (BDs) are among the most common objects in the Galactic field (e.g., Kroupa 2001; Chabrier et al. 2005). The majority of the neighbors of the Sun are BDs or are of spectral type M. Notably, the closest star to our Sun, Proxima Centauri, is an M-dwarf that orbits the α Cen A/B system. Our closest neighbors beyond this system are primarily of very low mass—including Barnard's star (Barnard 1916), the binary BD Luhman 16 (Luhman 2013), which may even have a third companion (Boffin et al. 2014), the BD WISE 0855-0714 (Luhman 2014), and many others, such as the M-stars Wolf 359 and Lalande 21185, as well as many BDs (e.g., Wolf 1919; Ross 1926; Luyten 1979; Strauss et al. 1999; Burgasser et al. 2004; Burningham et al. 2010; Kirkpatrick et al. 2013; Troup et al. 2016, and numerous others). Given their faintness, it is likely that future surveys will reveal the presence of even more nearby low-mass stars and BDs. Finally, approximately one quarter of the nearby low-mass neighbors of the Sun are known to host one or more companions (e.g., Burgasser et al. 2007; Luhman 2012; Duchêne & Kraus 2013; Ward-Duong et al. 2015), while many others are companions to higher-mass stars (see, e.g., Kouwenhoven 2006, and references therein).

Despite their ubiquity, the formation mechanism for low-mass objects, particularly BDs, is still poorly understood. It may be possible that BDs form from core collapse, similar to higher-mass stars (see, e.g., André et al. 2014; Riaz et al. 2014;

Lomax et al. 2015). However, their masses are below or close to the Jeans mass in star-forming regions (e.g., Palau et al. 2014; de Gregorio-Monsalvo et al. 2016). Another formation mechanism may be the gravitational fragmentation of circumstellar disks, and numerical simulations suggest that this is indeed possible (e.g., Stamatellos & Whitworth 2009a, 2009b; Tsukamoto et al. 2013; Forgan et al. 2015; Dong et al. 2016). What fraction of circumstellar disks fragment, however, is still unknown. The decay of such disk-fragmented systems results in a population of low-mass stars, BDs, and (free-floating) planetary-mass objects (PMOs) that contribute to shaping the low-mass end of the initial mass function (see, e.g., Thies & Kroupa 2007, 2008; Marks et al. 2015; Thies et al. 2015).

Disk fragmentation results in the formation of multiple secondaries around the central star with masses ranging from the planetary to the stellar regime. In this paper we follow the long-term (Gyr) dynamical evolution of such disk-fragmented systems, using the results of Li et al. (2015, hereafter L15) as initial conditions. Throughout this paper, we follow the classification of L15 by grouping the secondaries into three categories: (i) low-mass hydrogen-burning stars (LMSs) with masses over $80\,M_J$ (M_J is the mass of Jupiter), (ii) BDs with masses in the range $13-80\,M_J$, and (iii) PMOs with masses below $13\,M_J$. We assume that all of these secondaries formed through the same mechanisms in our simulations; however,

<div align="center">

Table 1
Initial Conditions for the Two Sets of Simulations

</div>

Quantity	Set 1	Set 2
Mass of host star	$M = 0.7\,M_\odot$	$M = 0.7\,M_\odot$
Notional disk mass	$M_{\rm d} \simeq 0.5\,M_\odot$	$M_{\rm d} \simeq 0.2\,M_\odot$
Number of secondaries	$4 \leqslant N \leqslant 11$	$3 \leqslant N \leqslant 5$
Mass of secondaries	$1\,M_{\rm J} \leqslant m \leqslant 200\,M_{\rm J}$	$1\,M_{\rm J} \leqslant m \leqslant 200\,M_{\rm J}$
	(at least one object with $m > 80\,M_{\rm J}$)	
Total mass of secondaries	$0.48\,M_\odot \leqslant m_{\rm tot} \leqslant 0.52\,M_\odot$	$0.18\,M_\odot \leqslant m_{\rm tot} \leqslant 0.22\,M_\odot$
Semimajor axis	$50\ {\rm au} < a < 350\ {\rm au}\ (m < 80\,M_{\rm J})$	$50\ {\rm au} < a < 250\ {\rm au}$
	$50\ {\rm au} < a < 150\ {\rm au}\ (m \geqslant 80\,M_{\rm J})$	
Eccentricity	$e = 0$	$e = 0$
Inclination	$0° < i < 5°$	$0° < i < 5°$
Longitude of the ascending node	$0° < \Omega < 360°$	$0° < \Omega < 360°$
Integration time	10 Myr (Stage I; L15)	10 Myr (Stage I; L15)
	10 Gyr (Stage II; this paper)	10 Gyr (Stage II; this paper)
Number of realizations	3000	6000

Note. The early evolution of the disk-fragmented systems up to 10 Myr is described in L15 and is referred to as Stage I. The long-term evolution, up to 10 Gyr, is discussed in this paper and is referred to as Stage II. The probability distributions of all parameters are described in L15.

each of these three categories may also form through other mechanisms (see Whitworth et al. 2007, p. 459; Luhman 2012).

L15 simulated the dynamical evolution of LMSs, BDs, and PMOs formed through disk fragmentation based on the outcomes of the smoothed particle hydrodynamical (SPH) simulations of Stamatellos & Whitworth (2009a). Their analysis covers the first 10 Myr of the dynamical evolution of these systems. They find that most systems attain a reasonably stable configuration at $t = 10$ Myr, after a large number of secondaries (mostly those with the lowest mass) have escaped. A non-negligible fraction of secondaries have paired up into low-mass binaries, many of which escape and some of which remain in orbit around their host star.

The simulations of L15 allow a comparison with observations of young stellar populations in or near star-forming regions and OB associations. For a comparison with the much older population of field stars, however, a further analysis is necessary. In this paper we therefore carry out N-body simulations of disk-fragmented systems up to 10 Gyr, covering the age range of most stars in the solar neighborhood.

This paper is organized as follows. We describe our methodology and initial conditions in Section 2. We describe our results in Section 3. Finally, we summarize and discuss our conclusions in Section 4.

2. METHOD AND INITIAL CONDITIONS

We study the long-term evolution of disk-fragmented systems using N-body simulations, following the methodology of L15. At time $t = 0$ Myr, each system in L15 initially consists of a host star of mass $0.7\,M_\odot$ and a varying number of low-mass secondaries. L15 studied the evolution of two types of disk-fragmented systems, which are referred to as set 1 and set 2. Set 1 uses the outcomes of the simulations of Stamatellos & Whitworth (2009a) to produce the initial conditions, while set 2 corresponds to the fragmentation of lower-mass disks, and allows evaluation of the robustness of the final results to the choice of initial conditions. The initial conditions for set 1 and set 2 are summarized in Table 1.

L15 study the evolution of disk-fragmented multiple systems for the first 10 Myr. In this paper we simulate the subsequent evolution of the systems up to 10 Gyr. We refer to the simulated time span in L15 ($t < 10$ Myr) as Stage I, and the

long-term evolution (10 Myr $< t <$ 10 Gyr) studied in this paper as Stage II. Stellar populations with ages corresponding to Stage I are typically observed in or near star-forming regions and OB associations, while Stage II is relevant for a comparison with the population of field stars.

Although we continue to study the evolution of all components of the systems up to $t = 10$ Gyr, it is not necessary to include the following in the N-body simulations: (i) host stars that are single at $t = 10$ Myr, (ii) systems that have a host star with only one bound companion at $t = 10$ Myr, and (iii) single or binary secondaries that have escaped before $t = 10$ Myr. As the above-mentioned objects do not experience any dynamical evolution after Stage I, they are not integrated, and are simply added to the data set after the N-body simulations of the other objects have finished. The final data sets thus contain 3000 systems (set 1) and 6000 systems (set 2).

We assume that all systems evolve in isolation. Encounters may alter the properties of multiple systems in the field, but close encounters are very rare in the low-density environment of the field (~ 0.1 systems pc^{-3}), and distant encounters will affect only the very widest systems.

We carry out the simulations of these systems using the MERCURY6 package (Chambers 1999). At the end of the simulations, at $t = 10$ Gyr, the energy conservation $\Delta E/E$ of all the systems is below (and usually well below) 10^{-3}. The identification of collisions, escapers, and binaries, as well as the determination of orbital elements, is carried out following the prescriptions of L15. We ignore the effects of stellar evolution, because none of the bodies in our systems has a mass high enough for stellar evolution to play a role within 10 Gyr.

We will see in Section 3 that at $t = 10$ Gyr the vast majority of the host stars have fewer than two bound companions, host stars with three companions are rare, and no host stars have more than three companions. To facilitate the discussion of our results, we refer to a host star with only a single bound companion as a *single-companion system*. When exactly two companions orbit the host star in separate orbits, we refer to the system as a *double-companion system*. If and only if a binary companion is in orbit around a host star, we refer to the system as a *binary-companion system*. In the last case, the two components of the binary are mutually gravitationally bound, and their mutual center of mass orbits the host star.
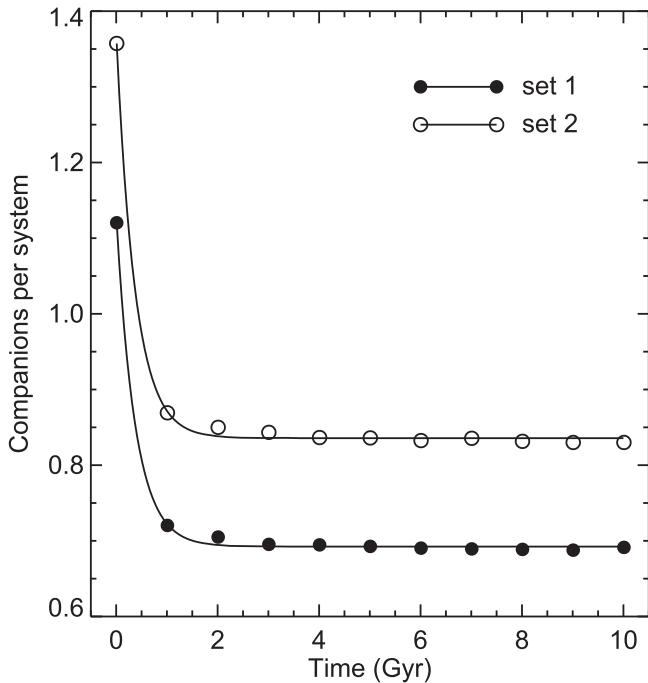
Figure 1. The number of bound secondary objects per system as a function of time for set 1 and set 2. The solid curves represent the best-fitting exponential decay curves for each data set.

3. RESULTS

3.1. Dynamical Decay of Disk-fragmented Systems

Although the duration of Stage I (0–10 Myr) is *much* shorter than that of Stage II (10 Myr–10 Gyr), most of the dynamically interesting events occur during Stage I.

For Stage II, Figure 1 shows the number of (gravitationally bound) companions per system as a function of time. During Stage II, the number of companions per host star decreases by 40% for both sets of initial conditions: from 1.12 to 0.69 for set 1, and from 1.36 to 0.83 for set 2. The number of companions mainly decreases during the first billion years. After this time, little further evolution occurs, and the remaining systems are mostly completely stable. In most cases, the asymptotic configuration of the system corresponds to either a single host star or a star with one companion. In a small fraction of cases, the dynamical interaction between the companions leads to a system with two or more companions in widely separated orbits, ensuring stability over long times.

All single host stars originate from the decay of systems in which a scattering event between two companions results in a nearly simultaneous combination of events: an ejection of one of the companions, and a collision between the other companion and the host star. An inspection of the data shows that this process is responsible for the origin of all of the 1110 single host stars in set 1 and all of the 1858 single host stars in set 2. In other words, all of the single host stars in our models are merger products. Table 4 presents the most important dynamical processes occurring in two representative systems in which the host star ultimately ends up single.

Although many of the results presented in the figures and tables in this paper correspond to the final configuration at 10 Gyr, the reader should keep in mind that evolution is slow beyond 1 Gyr, and that many of these results are therefore also good approximations for a stellar population with an age spread
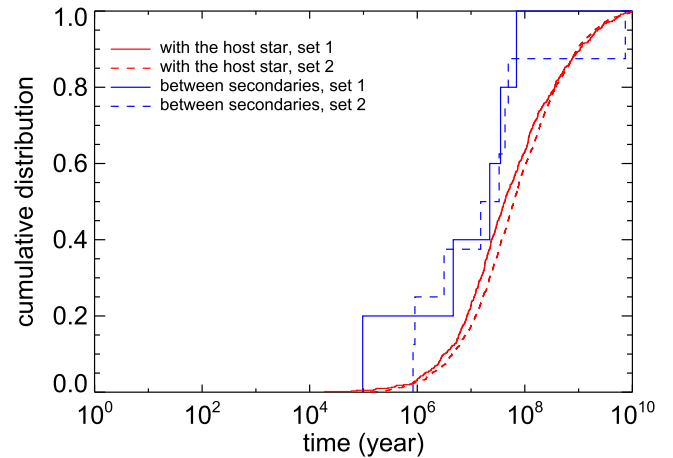
Figure 2. The cumulative distributions of the time of collisions with the host star (red) and between secondaries (blue) for set 1 (solid curves) and set 2 (dashed curves). The horizontal axis indicates the time relative to the start of Stage II.

similar to that of the solar neighborhood (i.e., only a small fraction of the stars are younger than 1 Gyr).

The data in Figure 1 can be fitted with an exponential decay function. We fit the average number of companions per system, $N(t)$, by

$$N(t) = (N_0 - N_\infty) \exp(-t/\lambda) + N_\infty, \tag{1}$$

where t is in units of Gyr. Here, N_0 is the value at the start of Stage II, and N_∞ represents the value the data sets approach when time becomes infinite, which is 0.70 and 0.84 companions per system for sets 1 and 2, respectively. Note that after 10 Gyr the average number of companions per primary is less than unity (among all companions that will eventually have disappeared at 10 Gyr, the half-life survival time is $t_{1/2} = \lambda \ln 2$, which is approximately 256 Myr for both sets of initial conditions).

Physical collisions between the host star and a companion or between companions continue to occur during Stage II. The distribution of the collision times during Stage II is shown in Figure 2. Almost all collisions between secondaries occur before 100 Myr, and about 90% of collisions with the host star occur within 1 Gyr. Few collisions occur beyond 1 Gyr because by that time most of the remaining systems have achieved a stable configuration. During Stage II, each host star experiences on average 0.20 collisions with a companion in set 1, and 0.25 collisions with a companion in set 2. The number of collisions between secondaries is substantially smaller: 0.0017 per system for set 1, and 0.0013 per system for set 2.

The collision rate during Stage II is substantially lower than that during Stage I, although Stage II lasts a thousand times longer. The reason for the much smaller rate of collisions during Stage II is twofold. First, there are fewer companions in the systems during Stage II. Second, the systems that have survived after Stage I are generally stable over long periods of time. Collisions with the host star occur much more frequently than collisions between secondaries. This is because the former require a strong perturbation of one (rather than two) of the companions, while the latter require a direct physical hit between two secondaries, which occurs less frequently.

The configurations of the systems at $t = 10$ Gyr are summarized in Table 2. By this time, almost all PMOs have
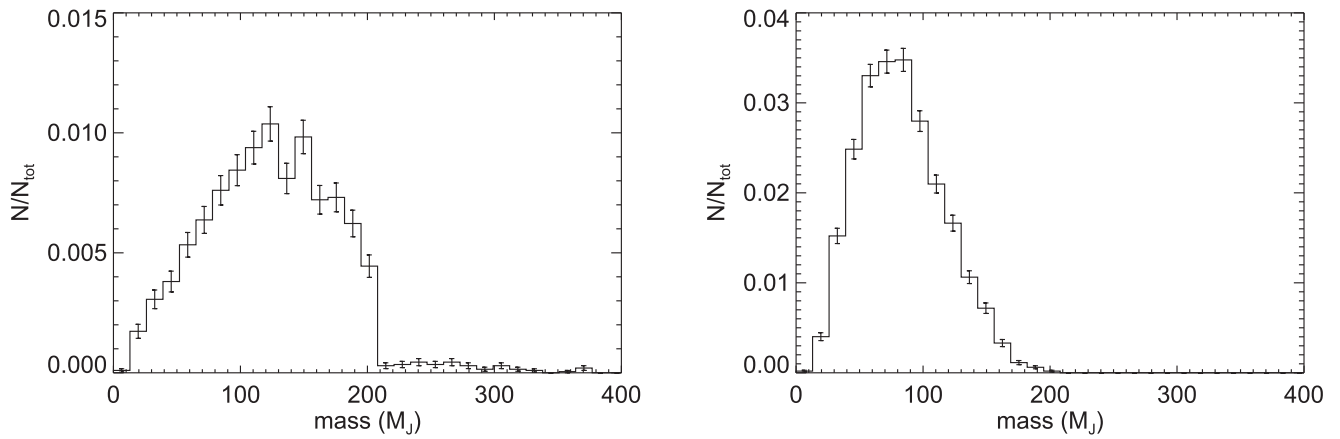
Figure 3. The mass distribution of bound secondary objects at $t = 10$ Gyr for set 1 (left) and set 2 (right) with Poissonian errors indicated. The distributions are normalized to the total number of secondaries at $t = 10$ Gyr.

Table 2
Statistical Properties of the Systems at $t = 10$ Gyr

Properties at $t = 10$ Gyr	Set 1	Set 2
Average number of companions per system	0.69	0.83
Single host stars	37%	31%
Host stars with 1 secondary	57%	55%
Host stars with 2 secondaries	5.9%	14%
Host stars with 3 secondaries	0.13%	0.03%
Host stars with $\geqslant 4$ secondaries	none	none
Bound single companions per system	0.67	0.81
Bound single PMOs per system	<0.001	<0.001
Bound single BDs per system	0.14	0.40
Bound single LMSs per system	0.53	0.41
Bound binary companions per system	0.011	0.008
Bound PMO–PMO binary companions per system	none	none
Bound PMO–BD binary companions per system	none	none
Bound PMO–LMS binary companions per system	none	none
Bound BD–BD binary companions per system	<0.001	0.003
Bound BD–LMS binary companions per system	0.002	0.005
Bound LMS–LMS binary companions per system	0.008	<0.001
Fraction of PMOs bound to host star	0.5%	0.7%
Fraction of BDs bound to host star	3.2%	14.7%
Fraction of LMSs bound to host star	25.8%	67.1%
Binary fraction among bound secondaries	1.6%	1.0%

Note. The total number of systems modeled is 3000 for set 1 and 6000 for set 2. A comparison with Table 2 in L15 shows that the systems continue to decay during Stage II, although, given the long time span of Stage II, the decay rate is substantially smaller than during Stage I.

Table 3
Average Number of Closely Bound PMOs, BDs, and LMSs per System at $t = 10$ Gyr (See Table 3 in L15).

Close Secondaries at $t = 10$ Gyr		Set 1	Set 2
Bound PMOs per system	$a \leqslant 10$ au	none	none
	$a \leqslant 20$ au	none	none
	$a \leqslant 50$ au	none	none
Bound BDs per system	$a \leqslant 10$ au	0.030	0.0037
	$a \leqslant 20$ au	0.045	0.048
	$a \leqslant 50$ au	0.051	0.24
Bound LMSs per system	$a \leqslant 10$ au	0.043	none
	$a \leqslant 20$ au	0.24	0.0012
	$a \leqslant 50$ au	0.37	0.14

during the fragmentation process. Figure 3 shows the mass distribution of secondaries that remain bound up to $t = 10$ Gyr. A comparison with Figures 1 and 3 in L15 shows that ejection probabilities are higher for lower-mass secondaries. High-mass secondaries have a high retention rate (see also Table 2), because ejection of such bodies almost requires a strong dynamical interaction with an even higher-mass secondary. Physical collisions between high-mass bodies result in the formation of merger products with masses beyond the range of our initial conditions (200 M_J), and most of these mergers occur during Stage I.

A comparison between the results at $t = 10$ Myr (Table 2 in L15) and the results at $t = 10$ Gyr (Table 2 in this paper) indicates a further decay of systems with two or more companions. Although all systems initially (at $t = 0$) had a large number of companions (3–11), roughly one third (37% for set 1 and 31% for set 2) of the host stars are single at $t = 10$ Gyr. About half of the host stars (57% for set 1 and 55% for set 2) have one companion left, and will therefore remain stable for very long periods of time, although they may ultimately be disrupted following a close encounter with a neighboring field star. A relatively small fraction of the systems remain in a triple system: 5.9% for set 1 and 14% for set 2. Among these, most consist of two companions orbiting the host star, although in several occasions the two companions formed a binary that orbits the host star (see Section 3.3). Very few host stars are quadruples, and there are no quintuples or higher-order systems. During Stage II the fraction of host stars with

escaped from their host star for both set 1 and set 2, or in rare cases, they have merged with the host star or another companion. Only 3.2% (set 1) and 14.7% (set 2) of the BDs that formed in the fragmented circumstellar disk remain bound to the host star. Compared with the PMOs and BDs, LMSs have a substantially higher chance of remaining in orbit around the host star: 25.8% (set 1) and 67.1% (set 2) of the LMSs formed in the circumstellar disk still orbit the host star at $t = 10$ Gyr.

The relatively high retention rate in set 2 is a result of the smaller number of (usually lower-mass) secondaries formed

Table 4
Evolution of Two Representative Systems that Fully Decay into Single Host Stars

Object	m_{initial} ($M_\odot$)	m_{final} ($M_\odot$)	Remarks
Star 2600 (set 1)	0.700	0.913	Merges with Comp. 1 (+3) at $t = 512$ kyr
Comp. 1	0.109	⋯	Merges with host star at $t = 512$ kyr
Comp. 2	0.112	0.112	Ejected
Comp. 3	0.104	⋯	Merges with Comp. 1 at $t = 2.313$ kyr
Comp. 4	0.083	0.083	Ejected at $t = 512$ kyr after scattering Comp. 1
Comp. 5	0.074	0.074	Ejected
Star 5999 (set 2)	0.700	0.798	Merges with Comp. 3 at $t = 16.75$ Myr
Comp. 1	0.071	0.071	Ejected at $t = 16.75$ Myr after scattering Comp. 3
Comp. 2	0.020	0.020	Ejected
Comp. 3	0.098	⋯	Merges with host star at $t = 16.75$ Myr

Note. For each of the components (Comp.) in the system the initial mass ($t = 0$ Gyr; start of Stage I) and the final mass ($t = 10$ Gyr; end of Stage II) are listed. The final scattering event results in the ejection of one companion and a merger between the other companion and the host star. All other ejections occur prior to this event.

zero or one companion increases over time: all host stars with zero or one companion at the beginning of Stage II remain as such, while other systems may decay into these.

By the end of Stage II approximately 1% of the host stars are accompanied by two companions in a binary configuration, of which the mutual center of mass orbits the host star. The average number of single companions per system is 0.67 for set 1 and 0.81 for set 2. For set 1 most of the companions are LMSs, while for set 2 roughly half of the single companions are LMSs while the other half are BDs. This difference can be attributed to the smaller initial number of companions as well as the steeper initial mass distribution of companions in set 2, which has resulted in fewer dynamical ejections of BDs. The average number of PMOs is negligible in both data sets, partially because of the preferred dynamical ejections of PMOs and partially because of the relatively small number of PMOs that have formed through disk fragmentation.

The number of close companions per system at $t = 10$ Gyr is shown in Table 3. At $t = 10$ Myr, no close ($\leqslant 50$ au) PMOs were present, and this number remains zero throughout Stage II. During Stage II, for set 1 the number of close BDs decreases by a little less than 50%, and the number of close LMSs decreases by about 25%. As the number of close BDs decreases more strongly than the number of close LMSs, the BD desert (Marcy & Butler 2000; Grether & Lineweaver 2006; Kouwenhoven et al. 2007; Kraus et al. 2008, 2011; Sahlmann et al. 2011) of set 1 becomes more prominent at the end of Stage II than it is at the end of Stage I.

3.2. Orbital Periods and Period Ratios

The distributions of the orbital periods of the companions at $t = 10$ Gyr are shown in Figure 4 for the three types of systems: single-companion systems, double-companion systems, and binary-companion systems. For each system (and subsystem, when applicable) we obtain the orbital elements. These include the *internal orbital elements* of the orbit of two secondaries orbiting a mutual center of mass, and the *external orbital elements* of this mutual center of mass around the host star.

In the single-companion systems, most LMSs tend to have shorter orbital periods than the BDs in set 1, while the periods of the LMSs and BDs are very similar in set 2, which is a result of the different initial distributions of semimajor axis. For set 1, the largest initial semimajor axis for LMSs is 150 au, but the value for BDs is 350 au. For set 2, on the other hand, the LMSs and BDs have a nearly identical range of initial semimajor axis.

In the double-companion systems, about 80% of the inner companions have periods within the range $P_{\text{in}} = 10$–1000 yr, and about 80% of the outer companions have orbital periods between $P_{\text{out}} = 1000$ yr and $P_{\text{out}} = 1$ Myr, for set 1. For set 2, about 90% of the inner companions have periods in the range $P_{\text{in}} = 100$–1000 yr, and about 90% of the outer companions have periods between $P_{\text{out}} = 1000$ yr and $P_{\text{out}} = 0.1$ Myr.

In the binary-companion systems, about 85% of the internal periods are between $P_{\text{int}} = 1$ yr and $P_{\text{int}} = 100$ yr, and about 85% of the external periods are in the range 100–10,000 yr, for set 1. About 75% of the internal periods are between $P_{\text{int}} = 10$ yr and $P_{\text{int}} = 100$ yr, and about 95% of the external periods are between $P_{\text{ext}} = 100$ yr and $P_{\text{ext}} = 10,000$ yr, for set 2.

The long-term stability of hierarchical systems consisting of three or more components is determined to first order by how well the different orbits in the system are gravitationally separated from each other. Figure 5 shows the distribution of orbital period ratios of double-companion systems and binary-companion systems. About 95% of the period ratios of double-companion systems are between $P_{\text{out}}/P_{\text{in}} = 10$ and $P_{\text{out}}/P_{\text{in}} = 10,000$, which means that the inner and outer orbits are usually very well separated. About 95% of the period ratios of binary-companion systems are in the range $P_{\text{ext}}/P_{\text{int}} = 10$–1000. These period ratios are generally large enough to ensure stability of these systems over billions of years.

### 3.3. Binarity among Companions in Multiple Systems

Although binary companions are not very common at $t = 10$ Gyr, they are dynamically very interesting. The internal and external distributions of the mass ratios, eccentricities, and inclinations of these binary companions are shown in Figure 6 for both set 1 (solid curves) and set 2 (dashed curves).

For the systems with a host star of mass M and binary companion components of masses m_1 and m_2 (with $M > m_1 \geqslant m_2$) we define the internal mass ratio as $q_{\text{int}} \equiv m_2/m_1$ and the external mass ratio as $q_{\text{ext}} \equiv (m_1 + m_2)/M$. The secondaries are generally of much lower mass than the host stars, so the distributions of internal mass ratios are peaked at higher values than those of external mass ratios for both set 1 and set 2. The median internal mass ratio is $q_{\text{int}} \approx 0.8$ for set 1 and $q_{\text{int}} \approx 0.6$ for set 2. The initial conditions and subsequent dynamical evolution are responsible for the higher values of the distributions of both the internal and external mass ratios in set 1 with respect to those in set 2. From an observational point of view, these relatively high mass ratios mean that these binary companions should be relatively easily observable. The
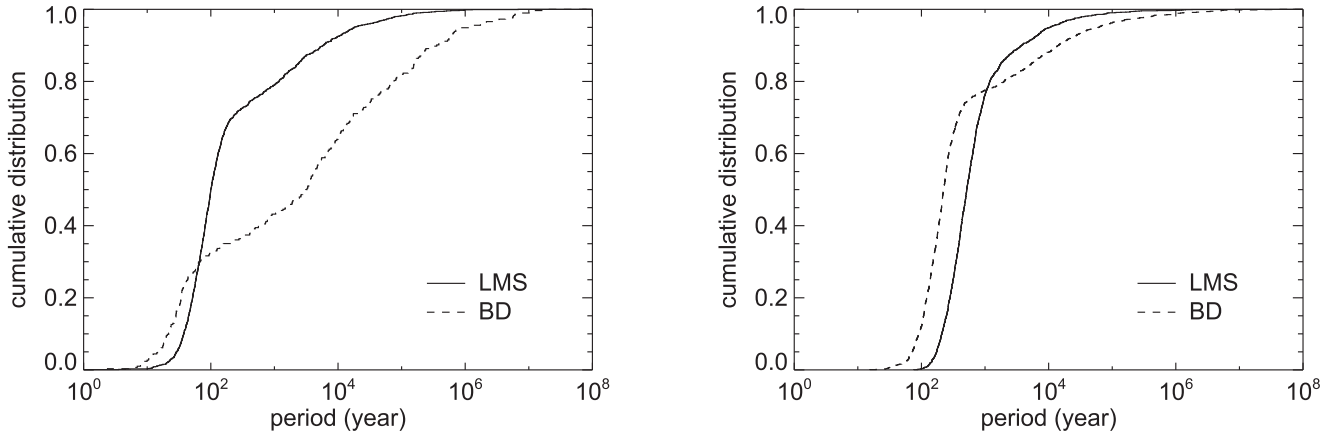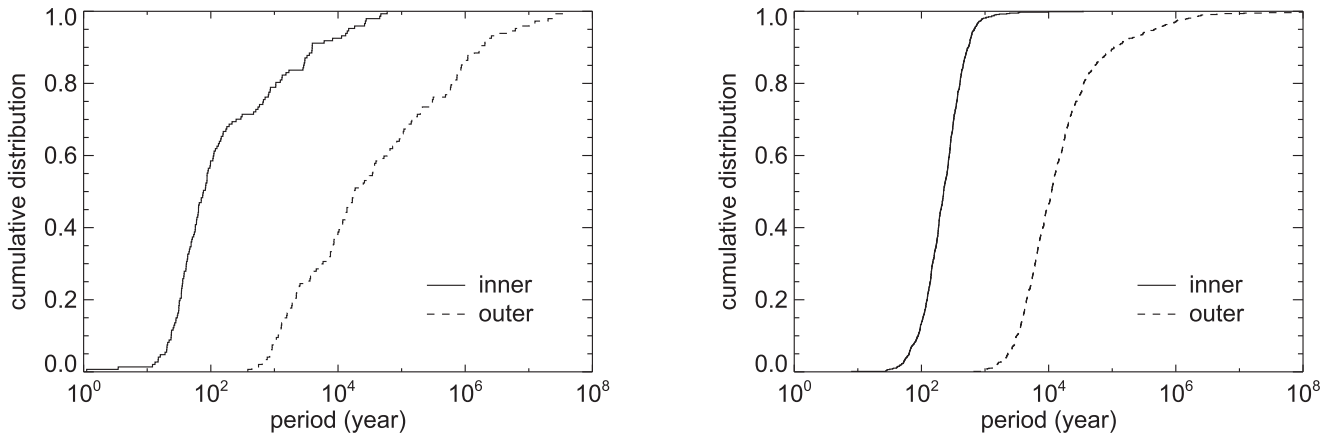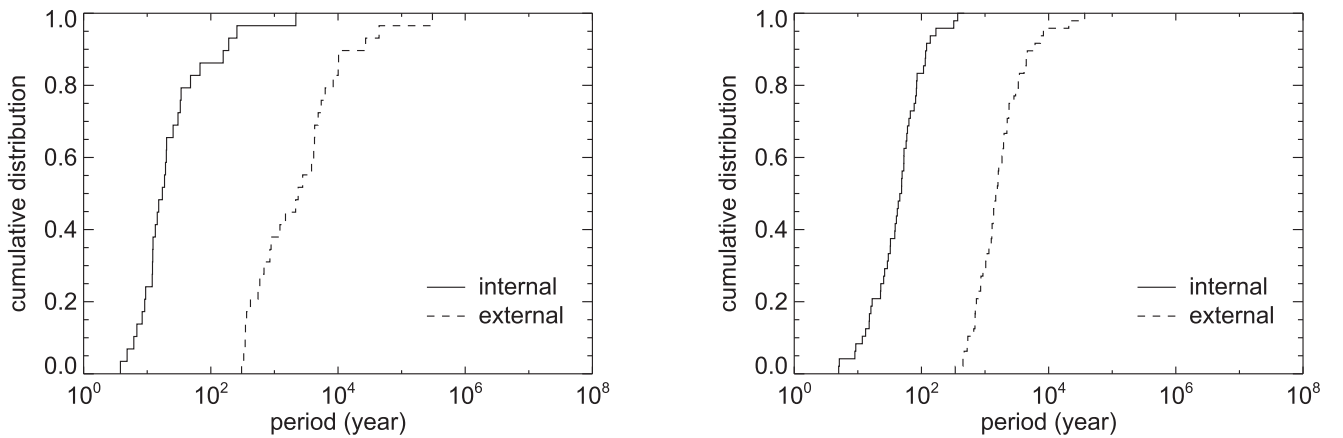
Figure 4. Orbital periods of the companions at $t = 10$ Gyr for set 1 (left) and set 2 (right). Top: cumulative period distributions of the LMSs (solid curves) and BDs (dashed curves) in single-companion systems. Middle: cumulative period distributions of inner companions (solid curves) and outer companions (dashed curves) in double-companion systems. Bottom: internal (solid curves) and external (dashed curves) cumulative period distributions in binary-companion systems.

external mass ratios are typically $q_{ext} = 0.15$–0.40 and the total mass of the binary companions is therefore typically $m_1 + m_2 = 0.1$–$0.3\ M_\odot$.

The distributions of internal and external eccentricity of the bound binary companions cover the whole range of eccentricities, with the exception of very small ($e \lesssim 0.05$) and very large ($e \gtrsim 0.95$) values. The distributions of internal eccentricity $f(e_{int})$ of both set 1 and set 2 are similar to the thermal distribution of eccentricity $f(e_{int}) = 2e_{int}$ (Heggie 1975). The external orbits are less eccentric, which is a result of the
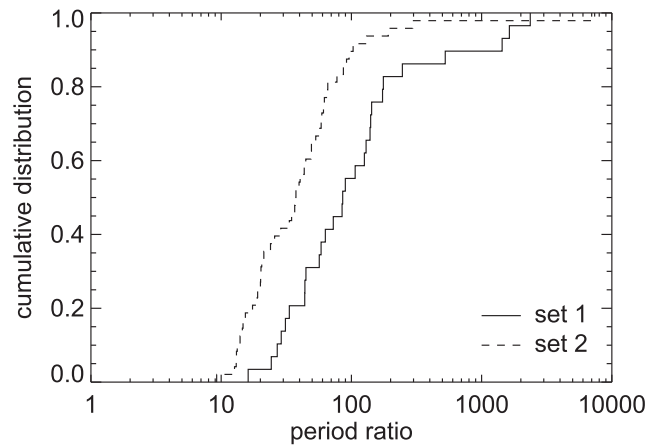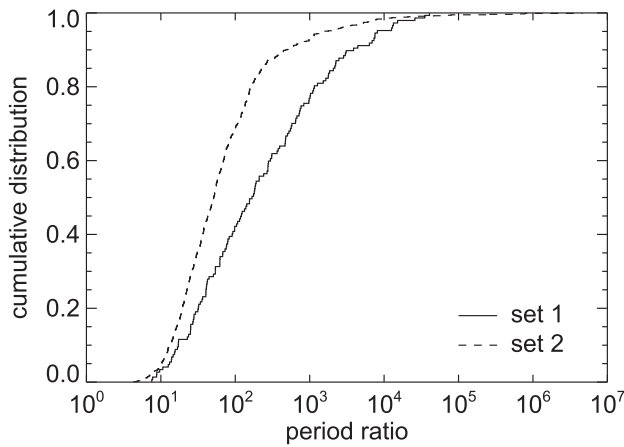
Figure 5. The distribution of period ratios of double-companion systems (left) and binary-companion systems (right) for set 1 (solid curves) and set 2 (dashed curves) at $t = 10$ Gyr (see Figure 4).

relatively large amount of orbital angular momentum that has to be conserved when two companions pair into a binary. Other secondaries interacting with the two secondaries in a binary companion during or after its formation may remove angular momentum from the binary companion. Hence, set 1, which has more companions than set 2 at the start of Stage I, displays an external distribution of eccentricity with, on average, higher eccentricities.

The bottom panel in Figure 6 shows the distributions of internal inclination $f(i_{int})$ and external inclination $f(i_{ext})$ for the binary companions in set 1 and set 2. All inclinations are measured with respect to the plane of the disk in which the secondaries were formed. For a hypothetical ensemble of completely randomly oriented orbits in space, the distribution of inclinations is $f(i) = \frac{1}{2}(1 - \cos i)$. In such configurations, half of the orbits have inclinations larger than 90°, i.e., they are retrograde. A brief inspection of Figure 6 shows that the distributions of both internal and external inclination are far from random. Most of the binary companions orbit their host star close to the plane of the disk in which they formed: approximately half of the external inclinations of the binary companions are below $i_{ext} = 20°$ in set 1 and half are below $i_{ext} = 10°$ in set 2. Again, the differences between the two data sets are a result of the larger initial number of secondaries in set 1 that resulted in more dynamical interactions, and therefore typically higher inclinations. Most of the binary companions have internal inclinations larger than $i_{int} = 90°$, which means that these binaries have retrograde orbits with respect to their orbit around the host star. This was also observed at the end of Stage I (see L15), and is mainly due to the fact that these retrograde binary companions form more easily because of angular momentum conservation. In addition, these systems are more stable than prograde binary companions, as can be seen by comparing the bottom panel in Figure 6 with Figure 15 in L15. The large spread in both the internal and external inclinations of the binary companions during Stage II suggests that for a subset of the systems the Kozai mechanism (Kozai 1962) is responsible for large variations in both eccentricity and inclination, partially accounting for the further disruption of the disk-fragmented systems at times beyond 1 Gyr. Therefore, non-alignment of the internal orbits of a hierarchical triple system does not necessarily provide evidence against formation in a disk. Thus, triple systems with orbits in the same plane, such as, e.g., Kepler-444 (Dupuy et al. 2016)

may not be that common, even if a large fraction of triple systems form by disk fragmentation.

4. CONCLUSIONS AND DISCUSSION

We have studied the long-term evolution of disk-fragmented systems, in order to study the orbital configurations of LMSs, BDs, and PMOs orbiting solar-type stars. This extends the simulations of L15 to cover 10 Gyr of dynamical evolution, which allows us to compare the products of the disk-fragmentation process with the field population in the solar neighborhood. We refer to the time span studied by L15 as Stage I (0–10 Myr) and the time span in this paper as Stage II (10 Myr–10 Gyr). Stage I represents roughly the period of time that the systems spend in or near their natal environment (star-forming regions and OB associations), while Stage II allows us to compare our results with the stellar population in the Galactic field. Our main conclusions can be summarized as follows:

1. Systems continue to decay beyond 10 Myr due to the decay of higher-order systems and also to collisions between members of the system. Almost all of this dynamical evolution occurs in the first billion years, leaving a very stable population after this time.

2. For approximately one third of the primaries (37% in set 1 and 31% in set 2), the host star ends up as a single star, despite the large number of secondaries (3–11) present during the phase of disk fragmentation. More than half of the host stars have one low-mass companion at $t = 10$ Gyr, while 6% (set 1) to 14% (set 2) of the host stars have two companions. Only a small fraction ($\lesssim 0.1\%$) of the host stars have three companions left, while no host star is able to retain four or more of its companions.

3. The number of physical collisions with the host star is non-negligible during Stage II. On average, each host star experiences 0.20 collisions in set 1, while the value is 0.25 for set 2. On the other hand, physical collisions between secondaries are very rare (less than 0.002 collisions per system).

4. For all primaries that ultimately end up as a single star (37% in set 1 and 31% in set 2), the final dynamical process to occur is a scattering event involving two companions, which results in the dynamical ejection of
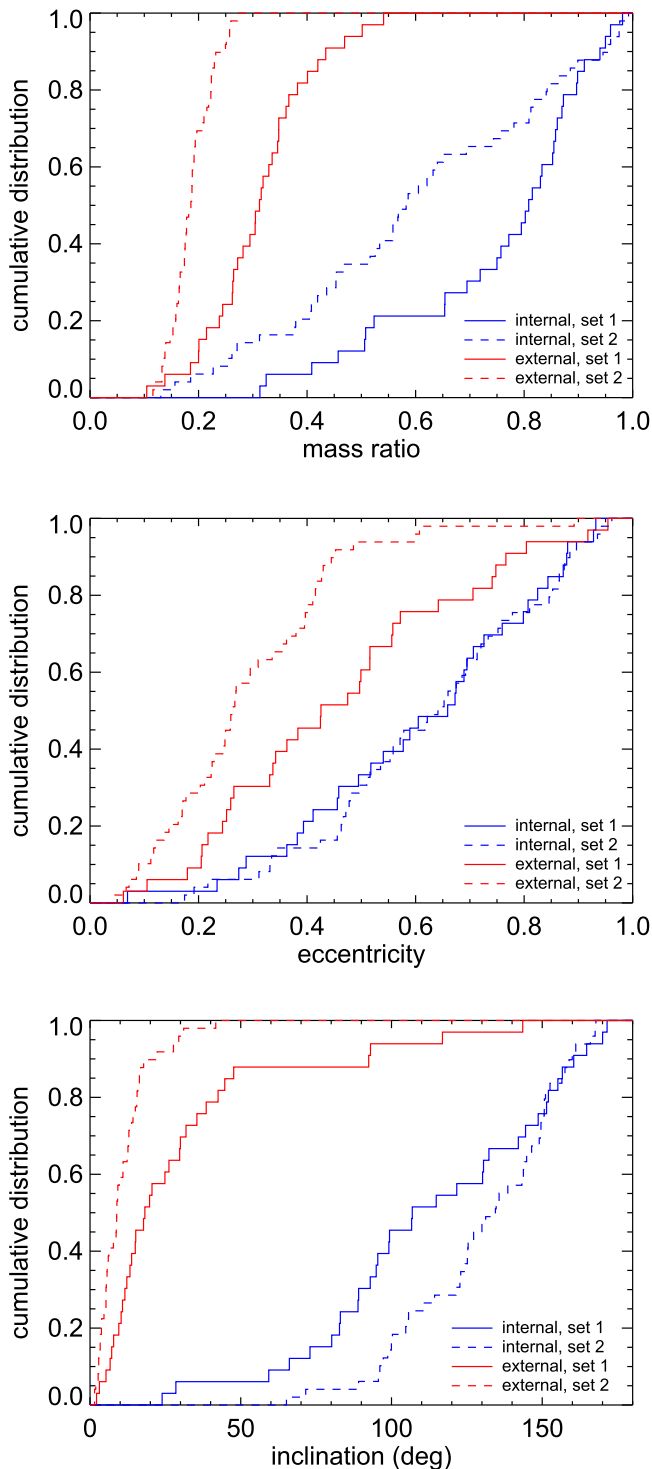
Figure 6. Cumulative distributions of orbital elements of the systems containing a bound binary companion: the mass ratios (top), binary eccentricities (middle), and binary inclinations (bottom) for set 1 (solid curves) and set 2 (dashed curves) at $t = 10$ Gyr. Blue and red curves represent internal and external results, respectively.

one of the companions and a merger between the host star and the other companion. All single host stars in our models are merger products.

5. At 10 Gyr, most of the remaining single companions orbit their host star in wide orbits with periods between 100 yr and 1 Myr (Figure 4). Very low-mass secondaries are potentially observable with imaging and radial velocity

surveys. PMOs with separations less than 50 au are absent, although higher-mass BDs and LMSs occur more frequently (ranging between, on average, 0.05 and 0.37 per system). The double-companion systems contain two companions that have widely separated orbits, with period ratios mostly ranging between $P_{out}/P_{in} = 10$ and $P_{out}/P_{in} = 10^4$.

6. Binary-companion systems orbiting the host star at $t = 10$ Gyr have external-to-internal period ratios mostly ranging between $P_{ext}/P_{int} = 10$ and 1000. The binary-companion masses are usually comparable, and the mass ratio of the binary system with respect to the host star is typically between $q_{ext} = 0.15$ and 0.40. The binary companions show a more or less thermal distribution of internal eccentricity (e_{int}), while their external eccentricities (e_{ext}) are on average smaller (although high eccentricities also exist among these external orbits). About half of the external inclinations of the binary companions are below $i_{ext} = 20°$ in set 1 and $i_{ext} = 10°$ in set 2, while a large majority of the binary companions have internal inclinations (i_{int}) beyond 90°, i.e., they have retrograde orbits.

Most nearby stars are low-mass stars or BDs that formed billions of years ago. Our study allows us to speculate somewhat on how these low-mass neighbors may have formed and evolved over time.

Disk fragmentation provides a possible (but certainly not the only) solution for the origin of many of these objects. The solar system itself is clearly a result of planet formation through core accretion. Also our closest neighbor, the triple system α Centauri, has likely formed differently, with its very low-mass companion Proxima Centauri perhaps being either a result of a capture event (e.g., Kouwenhoven et al. 2010; Moeckel & Clarke 2011; Parker & Meyer 2014) or a result of a triple decay event (e.g., Reipurth & Mikkola 2012). The other known objects with a distance smaller than that of Sirius are the very low-mass single objects Barnard's Star (Barnard 1916), WISE 0855-0714 (Luhman 2014), Wolf 359, and Lalande 21185, and the very low-mass binary system Luhman 16 (Luhman 2013). The nearby population beyond Sirius is also dominated by very low-mass objects. Although disk fragmentation may not be the dominant scenario responsible for the origin of this low-mass population, it does explain many of its properties, including the origin of the very low-mass binaries and multiples in the proximity of the Sun, such as Luhman 16, Luyten 726-8, EZ Aquarii, Struve 2398, Gloobridge 34, and Epsilon Indi.

Our study provides insight into a possible formation scenario for LMS, BD, and PMO companions to solar-type stars in the more distant Galactic field, as well as their free-floating siblings, both in the form of singles and binaries. Many stars in the Galactic field are part of a binary or of a hierarchical multiple system (e.g., Tokovinin & Smekhov 2002; Tokovinin 1997, 2008, 2014). As dynamical capture is rare, these systems are almost certainly formed as such. Our theory provides an excellent explanation for the origin of several hierarchical multiples, for example, the hierarchical triple systems HIP 68532 and HIP 69113, which both consist of a main-sequence star with a double companion made up of two low-mass stars (see Figure 9 in Kouwenhoven et al. 2005). The scarcity of close-in BD companions predicted by our model is also reflected in observations (e.g., Kouwenhoven et al. 2007).

A deeper analysis and more detailed comparison with observations is necessary, because with our simulations we have covered only a subset of all possible initial conditions that may lead to disk fragmentation. In addition, we have not taken into account the effect of encounters with neighboring stars and BDs, an effect that may be particularly important during the first few million years, when a disk-fragmented system is still in its dense natal environment where the circumstellar disk is initially exposed to the violent interstellar medium (e.g., Bik et al. 2010) and it subsequently participates in rapid exchange of energy with its neighbors (see, e.g., Allison et al. 2009 and numerous others). Stellar encounters can disrupt existing stellar and planetary systems (e.g., Wang et al. 2015a, 2015b, 2016; Zheng et al. 2015), although in the Galactic field this mostly affects the widest companions. In the case of systems with multiple companions, perturbations of outer companions can induce destabilization because the perturbation of an outer component can propagate to the inner system (e.g., Hao et al. 2013; Cai et al. 2015, 2016). The Galactic field itself also affects the evolution of wide binaries (e.g., Jiang & Tremaine 2010; Kaib et al. 2013). Finally, other stars and BDs in the environment may be captured by the host system following a close encounter, and previously escaped secondaries may be captured by other stars as well (e.g., Kouwenhoven et al. 2010; Perets & Kouwenhoven 2012), which may provide an alternative solution to the origin of wide, low-mass companions. The stars and BDs in the solar neighborhood likely represent a mixed population resulting from different formation mechanisms and from a different history of environmental interaction. Despite the many unknowns, our model makes clear predictions that can be compared statistically with nearby stars and BDs to further constrain their origin.

REFERENCES

Allison, R. J., Goodwin, S. P., Parker, R. J., et al. 2009, ApJL, 700, L99
André, P., Di Francesco, J., Ward-Thompson, D., et al. 2014, in Protostars and Planets VI, ed. H. Beuther et al. (Tucson, AZ: Univ. Arizona Press), 27
Barnard, E. E. 1916, AJ, 29, 181
Bik, A., Puga, E., Waters, L. B. F. M., et al. 2010, ApJ, 713, 883
Boffin, H. M. J., Pourbaix, D., Mužić, K., et al. 2014, A&A, 561, L4
Burgasser, A. J., McElwain, M. W., Kirkpatrick, J. D., et al. 2004, AJ, 127, 2856
Burgasser, A. J., Reid, I. N., Siegler, N., et al. 2007, in Protostars and Planets V, ed. B. Reipurth, D. Jewitt, & K. Keil (Tucson, AZ: Univ. Arizona Press), 427
Burningham, B., Pinfield, D. J., Lucas, P. W., et al. 2010, MNRAS, 406, 1885
Cai, M. X., Meiron, Y., Kouwenhoven, M. B. N., Assmann, P., & Spurzem, R. 2015, ApJS, 219, 31
Cai, M. X., Spurzem, R., & Kouwenhoven, M. B. N. 2016, in Proc. IAU Symp. 312, Star Clusters and Black Holes in Galaxies across Cosmic Time, ed. Y. Meiron et al. (Cambridge: Cambridge Univ. Press), 235
Chabrier, G., Baraffe, I., Allard, F., & Hauschildt, P. H. 2005, arXiv:astro-ph/0509798
Chambers, J. E. 1999, MNRAS, 304, 793
de Gregorio-Monsalvo, I., Barrado, D., Bouy, H., et al. 2016, A&A, 590, A79
Dong, R., Vorobyov, E., Pavlyuchenkov, Y., Chiang, E., & Liu, H. B. 2016, ApJ, 823, 141
Duchêne, G., & Kraus, A. 2013, ARA&A, 51, 269
Dupuy, T. J., Kratter, K. M., Kraus, A. L., et al. 2016, ApJ, 817, 80
Forgan, D., Parker, R. J., & Rice, K. 2015, MNRAS, 447, 836
Grether, D., & Lineweaver, C. H. 2006, ApJ, 640, 1051
Hao, W., Kouwenhoven, M. B. N., & Spurzem, R. 2013, MNRAS, 433, 867
Heggie, D. C. 1975, MNRAS, 173, 729
Jiang, Y.-F., & Tremaine, S. 2010, MNRAS, 401, 977
Kaib, N. A., Raymond, S. N., & Duncan, M. 2013, Natur, 493, 381
Kirkpatrick, J. D., Cushing, M. C., Gelino, C. R., et al. 2013, ApJ, 776, 128
Kouwenhoven, M. B. N. 2006, PhD thesis, Ponsen & Looijen, Wageningen
Kouwenhoven, M. B. N., Brown, A. G. A., Portegies Zwart, S. F., & Kaper, L. 2007, A&A, 474, 77
Kouwenhoven, M. B. N., Brown, A. G. A., Zinnecker, H., Kaper, L., & Portegies Zwart, S. F. 2005, A&A, 430, 137
Kouwenhoven, M. B. N., Goodwin, S. P., Parker, R. J., et al. 2010, MNRAS, 404, 1835
Kozai, Y. 1962, AJ, 67, 591
Kraus, A. L., Ireland, M. J., Martinache, F., & Hillenbrand, L. A. 2011, ApJ, 731, 8
Kraus, A. L., Ireland, M. J., Martinache, F., & Lloyd, J. P. 2008, ApJ, 679, 762
Kroupa, P. 2001, MNRAS, 322, 231
Li, Y., Kouwenhoven, M. B. N., Stamatellos, D., & Goodwin, S. P. 2015, ApJ, 805, 116
Lomax, O., Whitworth, A. P., Hubber, D. A., Stamatellos, D., & Walch, S. 2015, MNRAS, 447, 1550
Luhman, K. L. 2012, ARA&A, 50, 65
Luhman, K. L. 2013, ApJL, 767, L1
Luhman, K. L. 2014, ApJL, 786, L18
Luyten, W. J. 1979, New Luyten Catalogue of Stars With Proper Motions Larger Than Two Tenths of an Arcsecond; and First Supplement (Minneapolis, MN: NLTT)
Marcy, G. W., & Butler, R. P. 2000, PASP, 112, 137
Marks, M., Janson, M., Kroupa, P., Leigh, N., & Thies, I. 2015, MNRAS, 452, 1014
Moeckel, N., & Clarke, C. J. 2011, MNRAS, 415, 1179
Palau, A., Zapata, L. A., Rodríguez, L. F., et al. 2014, MNRAS, 444, 833
Parker, R. J., & Meyer, M. R. 2014, MNRAS, 442, 3722
Perets, H. B., & Kouwenhoven, M. B. N. 2012, ApJ, 750, 83
Reipurth, B., & Mikkola, S. 2012, Natur, 492, 221
Riaz, R., Farooqui, S. Z., & Vanaverbeke, S. 2014, MNRAS, 444, 1189
Ross, F. E. 1926, AJ, 36, 124
Sahlmann, J., Ségransan, D., Queloz, D., et al. 2011, A&A, 525, AA95
Stamatellos, D., & Whitworth, A. P. 2009a, MNRAS, 392, 413
Stamatellos, D., & Whitworth, A. P. 2009b, MNRAS, 400, 1563
Strauss, M. A., Fan, X., Gunn, J. E., et al. 1999, ApJL, 522, L61
Thies, I., & Kroupa, P. 2007, ApJ, 671, 767
Thies, I., & Kroupa, P. 2008, MNRAS, 390, 1200
Thies, I., Pflamm-Altenburg, J., Kroupa, P., & Marks, M. 2015, ApJ, 800, 72
Tokovinin, A. 2008, MNRAS, 389, 925
Tokovinin, A. 2014, AJ, 147, 87
Tokovinin, A. A. 1997, A&AS, 124, 75
Tokovinin, A. A., & Smekhov, M. G. 2002, A&A, 382, 118
Troup, N. W., Nidever, D. L., De Lee, N., et al. 2016, AJ, 151, 85
Tsukamoto, Y., Machida, M. N., & Inutsuka, S.-i. 2013, MNRAS, 436, 1667
Wang, L., Kouwenhoven, M. B. N., Zheng, X., Church, R. P., & Davies, M. B. 2015a, MNRAS, 449, 3543
Wang, L., Spurzem, R., Aarseth, S., et al. 2015b, MNRAS, 450, 4070
Wang, L., Spurzem, R., Aarseth, S., et al. 2016, MNRAS, 458, 1450
Ward-Duong, K., Patience, J., De Rosa, R. J., et al. 2015, MNRAS, 449, 2618

Whitworth, A., Bate, M. R., Nordlund, Å., Reipurth, B., & Zinnecker, H. 2007, in Protostars and Planets V, ed. B. Reipurth, D. Jewitt, & K. Keil (Tucson, AZ: Univ. Arizona Press), 459

Wolf, M. 1919, VeHei, 7, 195
Zheng, X., Kouwenhoven, M. B. N., & Wang, L. 2015, MNRAS, 453, 2759